

## Dark matter annihilation at the galactic center

Paolo Gondolo

*Max Planck Institut für Physik, Föhringer Ring 6, 80805 Munich, Germany*

Email: gondolo@mppmu.mpg.de

Joseph Silk

*Astrophysics, University of Oxford, Keble Road, Oxford, OX1 3RH, U.K.*

and

*Department of Astronomy and Physics, University of California, Berkeley, CA 94720*

Email: silk@astro.ox.ac.uk

If cold dark matter is present at the galactic center, as in current models of the dark halo, it is accreted by the central black hole into a dense spike. Particle dark matter then annihilates strongly inside the spike, making it a compact source of photons, electrons, positrons, protons, antiprotons, and neutrinos. The spike luminosity depends on the density profile of the inner halo: halos with finite cores have unnoticeable spikes, while halos with inner cusps may have spikes so bright that the absence of a detected neutrino signal from the galactic center already places interesting upper limits on the density slope of the inner halo. Future neutrino telescopes observing the galactic center could probe the inner structure of the dark halo, or indirectly find the nature of dark matter.

The evidence is mounting for a massive black hole at the galactic center. Ghez et al. [1] have confirmed and sharpened the Keplerian behavior of the star velocity dispersion in the inner 0.1 pc of the galaxy found by Eckart and Genzel [2]. These groups estimate the mass of the black hole to be  $M = 2.6 \pm 0.2 \times 10^6 M_\odot$ .

If cold dark matter is present at the galactic center, as in current models of the dark halo, it is redistributed by the black hole into a cusp. We call it the central ‘spike,’ to avoid confusion with the inner halo cusp favored by present N-body simulations of galaxy formation [3]. If cold dark matter contains neutral elementary particles that can annihilate with each other, like the supersymmetric neutralino, the annihilation rate in the spike is strongly increased as it depends on the square of the matter density. The steep spike profile, with index  $\geq 3/2$ , then implies that most of the annihilations take place at the inner radius of the spike, determined either by self-annihilation or by capture into the black hole.

Of the annihilation end-products, neutrinos escape the spike and propagate to us undisturbed. Current limits on the neutrino emission from the galactic center place upper limits on the slope of the inner halo. Future neutrino telescopes may improve on these limits or bring information on the nature of dark matter.

### I. ADIABATIC SPIKE AROUND THE CENTRAL BLACK HOLE

We find the dark matter density profile in the region where the black hole dominates the gravitational potential. From the data in [1,2], this is the region  $r \lesssim R_M \simeq 0.2$  pc. Other masses (the central star cluster, for example) also influence the dark matter distribution,

but since they make the gravitational potential deeper, their effect is to increase the central dark matter density and the annihilation signals.

We work under the assumption that the growth of the black hole is adiabatic. This assumption is supported by the collisionless behavior of particle dark matter. We can find the final density after black hole formation from the final phase-space distribution  $f'(E', L')$  as

$$\rho'(r) = \int_{E'_m}^0 dE' \int_{L'_c}^{L'_m} dL' \frac{4\pi L'}{r^2 v_r} f'(E', L'), \quad (1)$$

with

$$v_r = \left[ 2 \left( E' + \frac{GM}{r} - \frac{L'^2}{2r^2} \right) \right]^{1/2}, \quad (2)$$

$$E'_m = -\frac{GM}{r} \left( 1 - \frac{4R_S}{r} \right), \quad (3)$$

$$L'_c = 2cR_S, \quad (4)$$

$$L'_m = \left[ 2r^2 \left( E' + \frac{GM}{r} \right) \right]^{1/2}. \quad (5)$$

We have neglected the contribution from unbound orbits ( $E' > 0$ ). The lower limit of integration  $L'_c$ , and the second factor in  $E'_m$ , are introduced to eliminate the particles with  $L < 2cR_S$  which are captured by the black hole. ( $R_S = 2GM/c^2$  is the Schwarzschild radius.) We relate  $f'(E', L')$  to the initial phase-space distribution  $f(E, L)$  through the relations, valid under adiabatic conditions,  $f'(E', L') = f(E, L)$ ,  $L' = L$ ,  $I'(E', L') = I(E, L)$ , where the last two equations are the conservation of the angular momentum  $L$  and of the radial action  $I(E, L)$ .

The density slope in the spike depends not only on the slope of the inner halo but also on the behavior of the initial phase-space density  $f(E, L)$  as  $E$  approaches the

potential at the center  $\phi(0)$  [4]. If  $f(E, L)$  approaches a constant, as in models with finite cores, the spike slope is  $\gamma_{\text{sp}} = 3/2$ . If  $f(E, L)$  diverges as  $[E - \phi(0)]^{-\beta}$ , as in models with an inner cusp, the spike slope is  $\gamma_{\text{sp}} > 3/2$ . Models with finite cores include [5]: the non-singular and the modified isothermal sphere, the Hénon isochrone model, the Plummer model, the King models, the modified Hubble profile, the Evans power-law models with  $R_c \neq 0$ , and the Zhao  $(\alpha, \beta, \gamma)$  models,  $\rho \sim r^{-\gamma}(1 + r^{1/\alpha})^{-\beta\alpha}$ , with  $\gamma = 0$  and  $1/(2\alpha) = \text{integer}$ . Models with an inner cusp include [5]: the models of Jaffe, Hernquist, Navarro-Frenk-White, the  $\gamma/\eta$  models of Dehnen and Tremaine et al., and the other Zhao models.

As an example of models with finite cores, we consider the isothermal sphere. It has  $f(E, L) = \rho_0(2\pi\sigma_v^2)^{-3/2} \exp(-E/\sigma_v^2)$ . Close to the black hole, we have  $E \ll \sigma_v^2$ , and  $f(E, L) \simeq \rho_0(2\pi\sigma_v^2)^{-3/2}$ , a constant. Then from eq. (1) we easily find

$$\rho'_{\text{iso}}(r) = \frac{4\rho_0}{3\sqrt{\pi}} \left( \frac{GM}{r\sigma_v^2} \right)^{3/2} \left( 1 - \frac{4R_S}{r} \right)^{3/2}, \quad (6)$$

valid for  $r \ll R_M \simeq 0.2$  pc. The last factor comes from the capture of particles by the black hole: the density vanishes for  $r < 4R_S$ .

As an example of models with an inner cusp, we consider a single power law density profile,  $\rho(r) = \rho_0(r/r_0)^{-\gamma}$ , with  $0 < \gamma < 2$ . Its phase-space distribution function is

$$f(E, L) = \frac{\rho_0}{(2\pi\phi_0)^{3/2}} \frac{\Gamma(\beta)}{\Gamma(\beta - \frac{3}{2})} \frac{\phi_0^\beta}{E^\beta}, \quad (7)$$

with  $\beta = (6 - \gamma)/[2(2 - \gamma)]$  and  $\phi_0 = 4\pi G r_0^2 \rho_0 / [(3 - \gamma)(2 - \gamma)]$ . To find  $f'(E', L')$ , we need to solve  $I'(E', L') = I(E, L)$  for  $E$  as a function of  $E'$ . In the field of a point-like mass, we have  $I'(E', L') = 2\pi [-L' + GM/\sqrt{-2E'}]$ . In the field of the power law profile, whose potential is proportional to  $r^{2-\gamma}$ , the action integral cannot be performed exactly. We have found an approximation good to better than 8% over all of phase space for  $0 < \gamma < 2$ :

$$I(E, L) = \frac{2\pi}{b} \left[ -\frac{L}{\lambda} + \sqrt{2r_0^2\phi_0} \left( \frac{E}{\phi_0} \right)^{\frac{4-\gamma}{2(2-\gamma)}} \right], \quad (8)$$

where  $\lambda = [2/(4 - \gamma)]^{1/(2-\gamma)} [(2 - \gamma)/(4 - \gamma)]^{1/2}$  and  $b = \pi(2 - \gamma)/B(\frac{1}{2-\gamma}, \frac{3}{2})$ . Expressing  $E$  as a function of  $E'$  and integrating eq. (1), we obtain

$$\rho'(r) = \rho_R g_\gamma(r) \left( \frac{R_{\text{sp}}}{r} \right)^{\gamma_{\text{sp}}}, \quad (9)$$

with  $\rho_R = \rho_0 (R_{\text{sp}}/r_0)^{-\gamma}$ ,  $\gamma_{\text{sp}} = (9 - 2\gamma)/(4 - \gamma)$ , and  $R_{\text{sp}} = \alpha_\gamma r_0 (M/\rho_0 r_0^3)^{1/(3-\gamma)}$ . For  $0 \leq \gamma \leq 2$ , the density slope in the spike,  $\gamma_{\text{sp}}$ , varies only between 2.25 and 2.5.

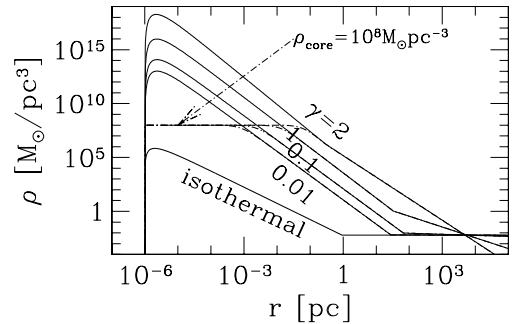


FIG. 1. Examples of spike density profiles.

While the exponent  $\gamma_{\text{sp}}$  can also be obtained by scaling arguments [4], the normalization  $\alpha_\gamma$  and the factor  $g_\gamma(r)$  accounting for capture must be obtained numerically. We find that  $g_\gamma(r) \simeq (1 - 4R_S/r)^3$  over our range of  $\gamma$ , and that  $\alpha_\gamma \simeq 0.293\gamma^{4/9}$  for  $\gamma \ll 1$ , and is  $\alpha_\gamma = 0.00733, 0.120, 0.140, 0.142, 0.135, 0.122, 0.103, 0.0818, 0.0177$  at  $\gamma = 0.05, 0.2, 0.4, \dots, 1.4, 2$ . The density falls rapidly to zero at  $r \lesssim 9.55R_S$ , vanishing for  $r < 4R_S$ .

Annihilations in the inner regions of the spike set a maximal dark matter density  $\rho_{\text{core}} = m/\sigma v t_{\text{bh}}$ , where  $t_{\text{bh}}$  is the age of the black hole, conservatively  $10^{10}$  yr,  $m$  is the mass of the dark matter particle, and  $\sigma v$  is its annihilation cross section times relative velocity (notice that for non-relativistic particles  $\sigma v$  is independent of  $v$ ). Using  $\partial\rho/\partial t = -\sigma v \rho^2/m$ , the final spike profile is

$$\rho_{\text{sp}}(r) = \frac{\rho'(r)\rho_{\text{core}}}{\rho'(r) + \rho_{\text{core}}}, \quad (10)$$

which has a core of radius  $R_{\text{core}} = R_{\text{sp}} (\rho_R/\rho_{\text{core}})^{1/\gamma_{\text{sp}}}$ . In the particle models we consider, not more than the initial amount of dark matter within 300 pc is annihilated.

Examples of spike density profiles are shown in Fig. 1.

To conclude this section, we derive a conservative estimate of the dark matter density near the galactic center. Assume that the halo density is constant on concentric ellipsoids. Then the halo contribution  $v_h(r)$  to the rotation speed at distance  $r$  fixes the halo mass within  $r$ . Assume further that the halo density decreases monotonically with distance. Since at large radii it decreases at least as fast as  $r^{-2}$ , and at small radii only as  $r^{-\gamma}$  with  $\gamma < 2$ , the density profile becomes steeper with distance. So to continue the  $r^{-\gamma}$  dependence to all radii keeping the same halo mass interior to  $r$  as given by the rotation speed, we must decrease the density normalization. In this way we obtain an underestimate of the density near the center. Letting  $\rho_D = \rho_0(D/r_0)^{-\gamma}$ , we have

$$\frac{\rho_D}{1 - \gamma/3} \sim \frac{3v_h^2(D)}{4\pi G D^2} \simeq 0.0062 \frac{M_\odot}{\text{pc}^3} \simeq 0.24 \frac{\text{GeV}}{\text{cm}^3}, \quad (11)$$

where we have taken  $v_h(D) = 90 \text{ km s}^{-1}$  at the Sun distance  $D = 8.5$  kpc, as obtained after subtracting a (somewhat overestimated) luminous matter contribution of  $180 \text{ km s}^{-1}$  to the circular speed of  $220 \pm 20 \text{ km s}^{-1}$  [6].

## II. SIGNALS FROM NEUTRALINO ANNIHILATIONS

Our analysis applies in general to a self-annihilating dark matter particle. To make it concrete, we examine a case of supersymmetric dark matter, the lightest neutralino. The minimal supersymmetric standard model provides a well-defined calculational framework, but contains at least 106 yet-unmeasured parameters [7]. Most of them control details of the squark and slepton sectors, and can safely be disregarded in dark matter studies. So we restrict the number of parameters to 7, following Bergström and Gondolo [8]. Out of the database of points in parameter space built in refs. [8–10], we use the 35121 points in which the neutralino is a good cold dark matter candidate, in the sense that its relic density satisfies  $0.025 < \Omega_\chi h^2 < 1$ . The upper limit comes from the age of the Universe, the lower one from requiring that neutralinos are a major fraction of galactic dark halos.

Gravitational interactions bring the cold neutralinos into our galactic halo and into the central spike, where neutralino pairs can annihilate and produce photons, electrons, positrons, protons, antiprotons, and neutrinos. While most products are subject to absorption and/or diffusion, the neutrinos escape the spike and propagate to us undisturbed. We focus on the neutrinos and postpone the study of other signals.

The expected neutrino flux from neutralino annihilations in the direction of the galactic center can be divided into two components: emission from the halo along the line of sight and emission from the central spike,

$$\Phi_\nu^{\text{neutralinos}} = \Phi_\nu^{\text{halo}} + \Phi_\nu^{\text{spike}}. \quad (12)$$

The halo flux from neutralino annihilations between us and the galactic center can be estimated assuming that a single power law profile  $\rho(r) = \rho_D (r/D)^{-\gamma}$  extends out to the Sun position  $r = D$ . The integrated neutrino flux within an angle  $\Theta$  of the galactic center is

$$\Phi_\nu^{\text{halo}} = \frac{\rho_D^2 Y_\nu \sigma v D \Omega(\Theta)}{m^2}, \quad (13)$$

where  $m$  is the neutralino mass,  $Y_\nu$  is the number of neutrinos produced per annihilation, either differential or integrated in energy,  $\sigma v$  is the neutralino–neutralino annihilation cross section times relative velocity, and

$$\Omega(\Theta) = \frac{\Theta^2}{2(1-2\gamma)} - \frac{2\gamma-1/2\Theta^{3-2\gamma}}{(3-2\gamma)(1-2\gamma)} - \frac{\Theta_{\min}^{3-2\gamma}}{3-2\gamma}. \quad (14)$$

Here  $\Theta$  is in radians and  $\Theta_{\min} = \max[10R_S/D, (2\gamma/3)^{1/(3-2\gamma)}(\rho_D/\rho_{\text{core}})^{1/\gamma}]$ .

We evaluate the neutrino yield  $Y_\nu$  and the neutralino annihilation cross sections  $\sigma$  using the DarkSUSY package [11], which incorporates Pythia simulations of the  $\nu$  continuum [12] and the annihilation cross sections in [9,13].

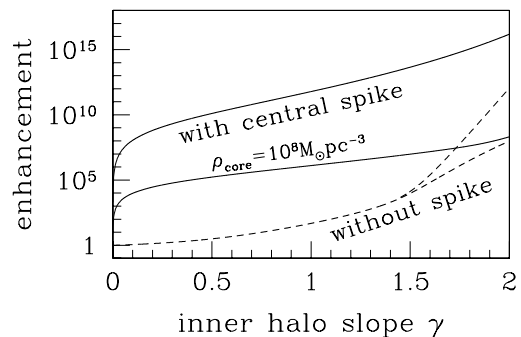


FIG. 2. Enhancement of annihilation signals from the galactic center.

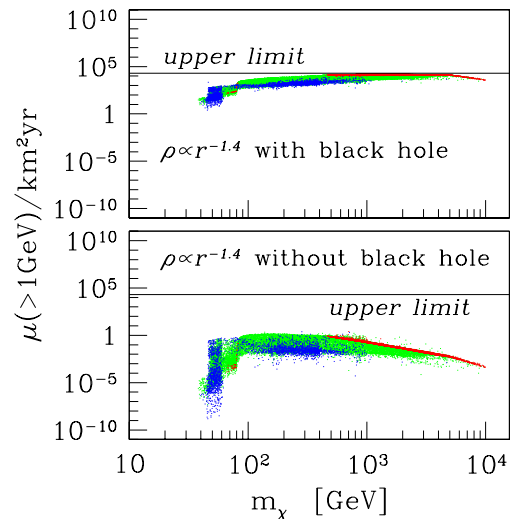


FIG. 3. For a Moore et al. halo profile, flux of neutrino-induced muons in a neutrino telescope from neutralino dark matter annihilations in the direction of the galactic center, with (upper panel) and without (lower panel) the central spike. The horizontal line is the current upper limit.

To the halo flux we need to add the contribution from the spike around the black hole at the galactic center. For an isothermal distribution we find

$$\Phi_\nu^{\text{spike}} = \frac{\rho_D^2 Y_\nu \sigma v D}{m^2} \left(\frac{R_M}{D}\right)^3 \ln\left(\frac{R_M}{25R_S}\right), \quad (15)$$

the factor of 25 serving to match the exact integration. This flux is a factor of  $\sim 10^{-9}$  smaller than the flux from dark matter annihilations between us and the galactic center, and so the addition of the spike does not modify the signal. The same conclusion is reached in general for halo models with finite cores.

A strong enhancement results instead for power law profiles. We find

$$\Phi_\nu^{\text{spike}} = \frac{\rho_D^2 Y_\nu \sigma v D}{m^2} \left(\frac{R_{\text{sp}}}{D}\right)^{3-2\gamma} \left(\frac{R_{\text{sp}}}{R_{\text{in}}}\right)^{2\gamma_{\text{sp}}-3}, \quad (16)$$

where  $R_{\text{sp}}$  is given after eq. (9) with  $\rho_0$  replaced by  $\rho_D$  and  $r_0$  by  $D$ . We fix  $R_{\text{in}}$  so as to match the inte-

gration of the numerically-calculated density profile including capture and annihilation: we find that  $R_{\text{in}} = 1.5 [(20R_S)^2 + R_{\text{core}}^2]^{1/2}$  gives a good approximation to the flux (within 6% for our values of  $\gamma$ ).

Contrary to the case of finite cores, for cusped halos there is a huge increase in flux from the galactic center when the spike is included, typically 5 orders of magnitude or more, unless the inner halo slope  $\gamma$  is very small (see Fig. 2, where  $\Theta = 1^\circ 5$ ). The enhancement is notable, for example, for the profile of Moore et al. which has  $\gamma = 1.4$  (see Fig. 3): including the spike around the black hole dramatically changes the prospects of observing a neutrino flux.

The neutrino flux from the spike increases with the inner halo slope  $\gamma$ . Imposing that it does not exceed the observed upper limit of  $\sim 2 \times 10^4$  muons( $> 1\text{GeV}$ )  $\text{km}^{-2} \text{yr}^{-1}$  [14] leads to an upper bound on  $\gamma$ . There is a separate upper bound for each model. They are plotted in Fig. 4a. (Plotted values of  $\gamma_{\text{max}} > 2$  are unphysical extrapolations but are shown for completeness.) Present bounds are of the order of  $\gamma_{\text{max}} \sim 1.5$ .

Future neutrino telescopes situated in the Northern hemisphere may improve on this bound or find a signal. For example, with a muon energy threshold of 25 GeV, the neutrino flux from the spike after imposing the current constraints could still be over 3 orders of magnitude above the atmospheric background (Fig. 5), allowing to probe  $\gamma$  as low as 0.05 (Fig. 4b).

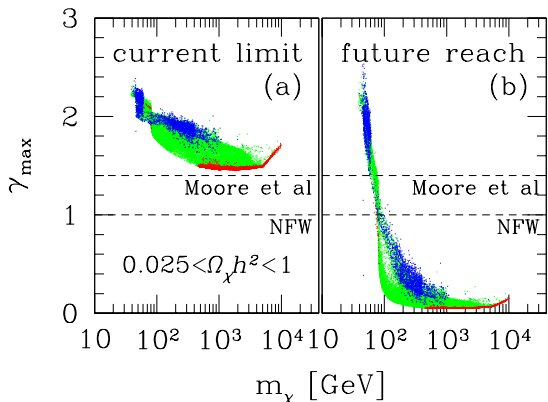


FIG. 4. Maximum inner slope  $\gamma$  of the dark matter halo compatible with the upper limit on the neutrino emission from the galactic center. (a) Current limit at 1 GeV; (b) future reach at 25 GeV.

In conclusion, we have shown that if the galactic dark halo is cusped, as favored in recent N-body simulations of galaxy formation, a bright dark matter spike would form around the black hole at the galactic center. A search of a neutrino signal from the spike could either set upper bounds on the density slope of the inner halo or clarify the nature of dark matter.

This research has been supported in part by grants from NASA and DOE.

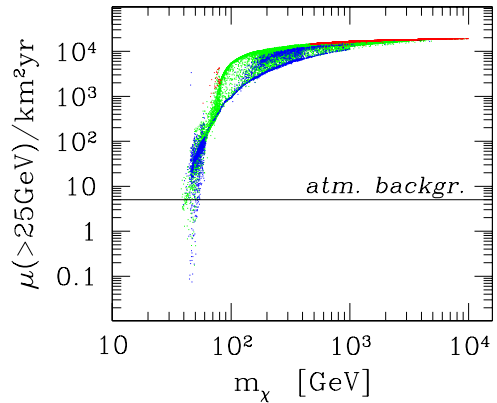


FIG. 5. Maximal flux of neutrino-induced muons in a neutrino telescope from neutralino annihilations at the galactic center, after imposing the current constraints on the neutrino emission.

- 
- [1] A. M. Ghez, B. L. Klein, M. Morris, and E. E. Becklin, *Ap. J.* **509**, 678 (1998).
  - [2] A. Eckart and R. Genzel, *Nature* **383**, 415 (1996); *MNRAS* **284**, 576 (1997).
  - [3] J. F. Navarro, C. Frenk, and S. White, *Ap. J.* **462**, 563 (1996); A. V. Kravtsov, A. A. Klypin, and A. M. Khokhlov, *Ap. J. Suppl.* **111**, 73 (1997); B. Moore et al., *Ap. J. Lett.* **499**, 5 (1998).
  - [4] G. D. Quinlan, L. Hernquist, and S. Sigurdsson, *Ap. J.* **440**, 554 (1995).
  - [5] See references in [4] and in J. Binney and S. Tremaine, *Galactic Dynamics* (Princeton Univ. Press, 1987); J. F. Navarro, C. Frenk, and S. White in [3]; N. W. Evans, *MNRAS* **267**, 333 (1994); H. S. Zhao, *MNRAS* **278**, 488 (1996).
  - [6] W. Dehnen and J. Binney, *MNRAS* **294**, 429 (1998) and references therein.
  - [7] S. Dimopoulos and D. Sutter, *Nucl. Phys.* **B465**, 23 (1995).
  - [8] L. Bergström and P. Gondolo, *Astropart. Phys.* **5**, 183 (1996).
  - [9] J. Edsjö and P. Gondolo, *Phys. Rev.* **D56**, 1879 (1997).
  - [10] L. Bergström, P. Ullio, and J. H. Buckley, *Astropart. Phys.* **9**, 137 (1998).
  - [11] P. Gondolo et al., unpublished.
  - [12] L. Bergström, J. Edsjö, P. Gondolo, and P. Ullio, *Phys. Rev.* **D59**, 043506 (1999).
  - [13] L. Bergström and P. Ullio, *Nucl. Phys.* **B504**, 27 (1997); Z. Bern, P. Gondolo, and M. Perelstein, *Phys. Lett.* **B411**, 86 (1997); P. Ullio and L. Bergström, *Phys. Rev.* **D57**, 1962 (1998).
  - [14] R. Svoboda et al., *Ap. J.* **315**, 420 (1987); Y. Oyama, et al., *Phys. Rev.* **D39**, 1481 (1989); H. Adarkar et al., *Ap. J.* **380**, 235 (1991); K. Nakamura, in *3rd NESTOR Int. Workshop*, Pylos, Greece, 1993.